Supplementary Materials

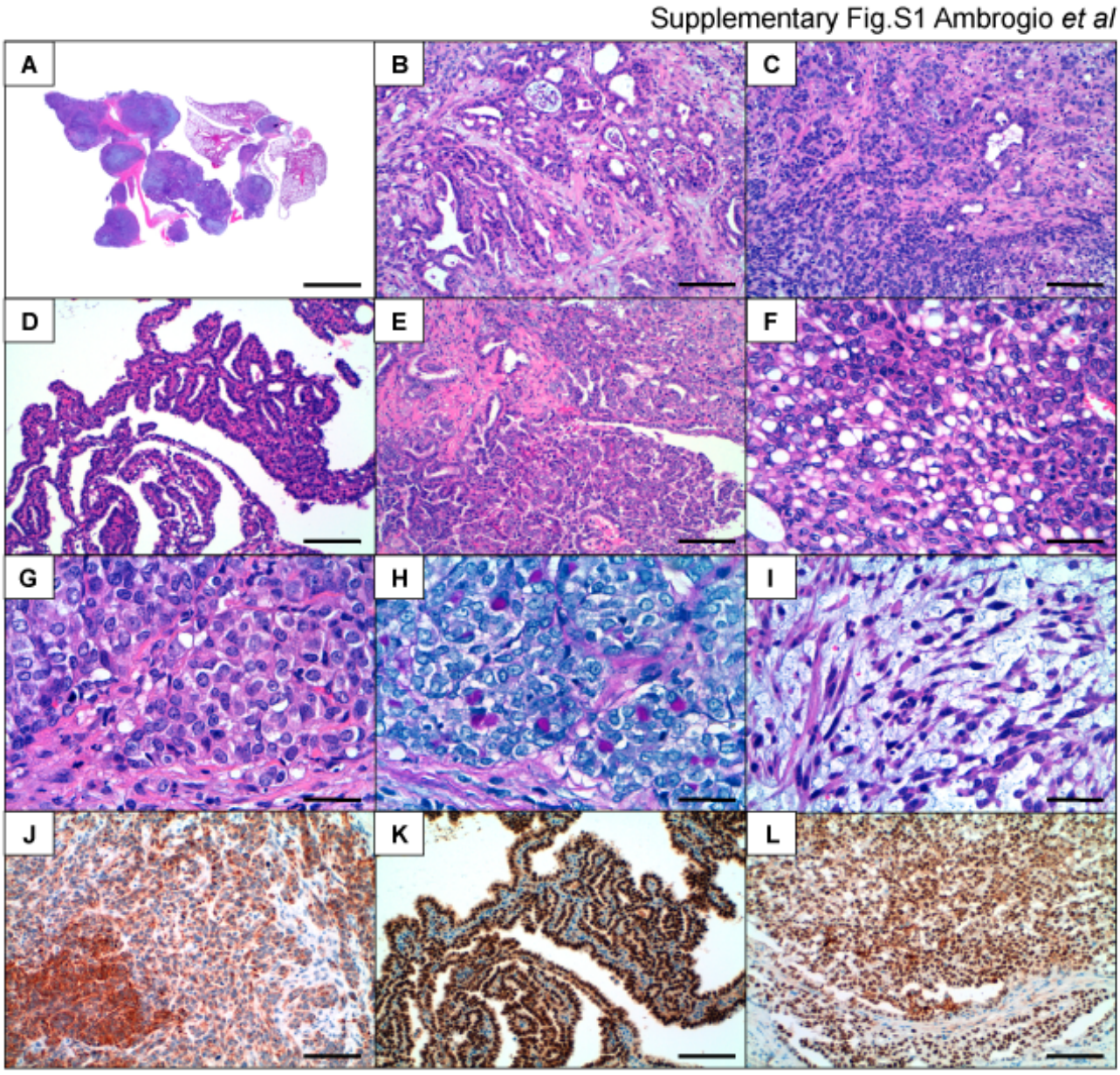

Fig. S1. Common histological subtypes of NSCLC orthoallografts.

Passage #1 orthoallografts derived from *K-Ras*$^{lox/LSLG12V}$; RERT$^{ert/ert}$ primary tumors after implantation into recipient nude mice. Engrafted tumors reproduce the major histological subtypes of human invasive lung adenocarcinoma. **A)** H&E staining of a representative engrafted tumor that shows invasion of the host lung. **B)** Acinar

adenocarcinoma consists of round to oval-shaped malignant glands invading a fibrous stroma. **C)** Papillary adenocarcinoma with contribution of solid adenocarcinoma. **D)** Pure papillary adenocarcinoma. **E)** Adenocarcinoma with areas of acinar and micropapillary subtypes. **F**) Adenocarcinoma with signet ring cell features. **G)** Solid adenocarcinoma with mucin component. **H)** Diastase-periodic acid Schiff (DPAS) staining to highlight the intracytoplasmatic mucin droplets in solid adenocarcinoma. **I)** Poorly differentiated adenocarcinoma with spindle cell features and sarcomatoid appearance. **J)** Cytokeratin 7 immunohistochemical staining in predominant solid adenocarcinoma with acinar component. **K)** Thyroid transcription factor-1 (TTF-1) immunohistochemical staining in papillary adenocarcinoma. **L)** TTF1 immunohistochemical staining in solid adenocarcinoma. Scale bars 100 µm except panel A (1 mm) and G, H, I (50 µm).

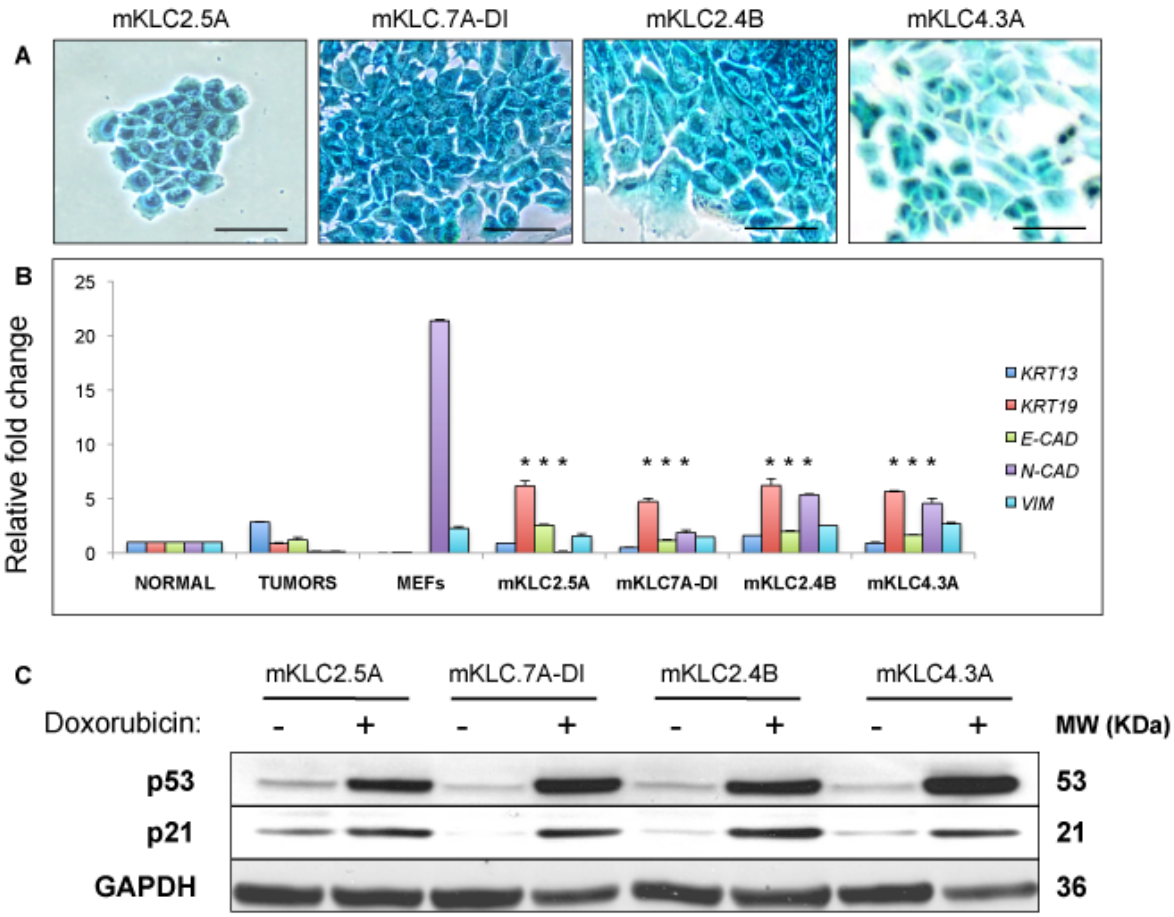

Fig. S2. *In vitro* characterization of primary cell lines derived from NSCLC orthoallografts.

A) Detection of K-Ras^{G12V} expression (based on its surrogate marker ß-Geo) by X-Gal staining in the indicated primary mKLC cell lines. Scale bar: 40 microns. **B)** qRT-PCR of the cytokeratins 13 and 19, N- and E-cadherin and vimentin in the indicated mKLC cell lines. Samples from murine normal lung, *K-Ras*$^{lox/LSLG12Vgeo}$ NSCLC primary tumors and mouse embryonic fibroblasts (MEFs) were assessed in parallel for comparative purposes. **C)** Western blot analysis of p53 and p21 in lysates prepared from the indicated mKLC cell lines in the presence or absence of doxorubicin. GAPDH is shown as a loading control. * indicates p-value < 0.01.

Supplementary Fig.S3 Ambrogio *et al*

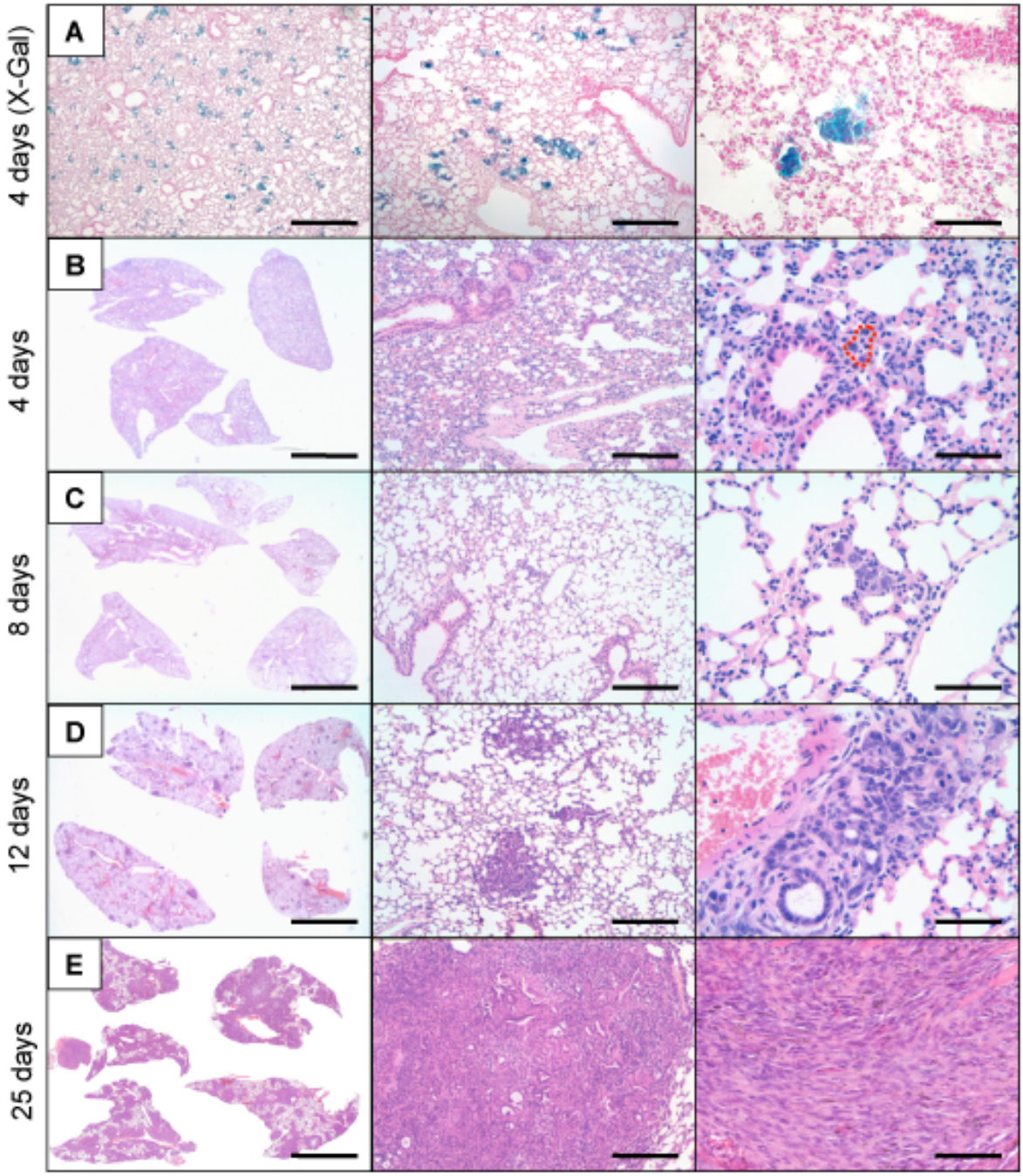

Fig. S3. Lung colonization and tumor formation upon reintroduction of mKLC cell lines.

A cohort of recipient nude mice (n=3 per time point) was inoculated with 10^6 mKLC cells (3 independent cell lines) via tail vein injection. Lung tissue was collected at 4, 8, 12, and 25 days post-injection and tissue sections stained with H&E **A)** X-Gal staining of lung sections after 4 days to facilitate detection of mKLC cells. **B)** Small clusters of tumor cells (marked by a red dashed line) were observed after 4 days. **C)** Presence of clusters of scattered atypical cells identified after 8 days. **D)** Small nodules of tumor cells with focal acinar differentiation observed at 12 days post-injection. **E)** Confluent tumor nodules including both acinar and solid components observed at humane end point (25 days after injection). Images of increasing magnification are shown from left to right, scale bars: left column 2 mm (except upper panel 400 µm), middle column 200 µm, right column 100 µm.

Supplementary Fig.S4 Ambrogio *et al*

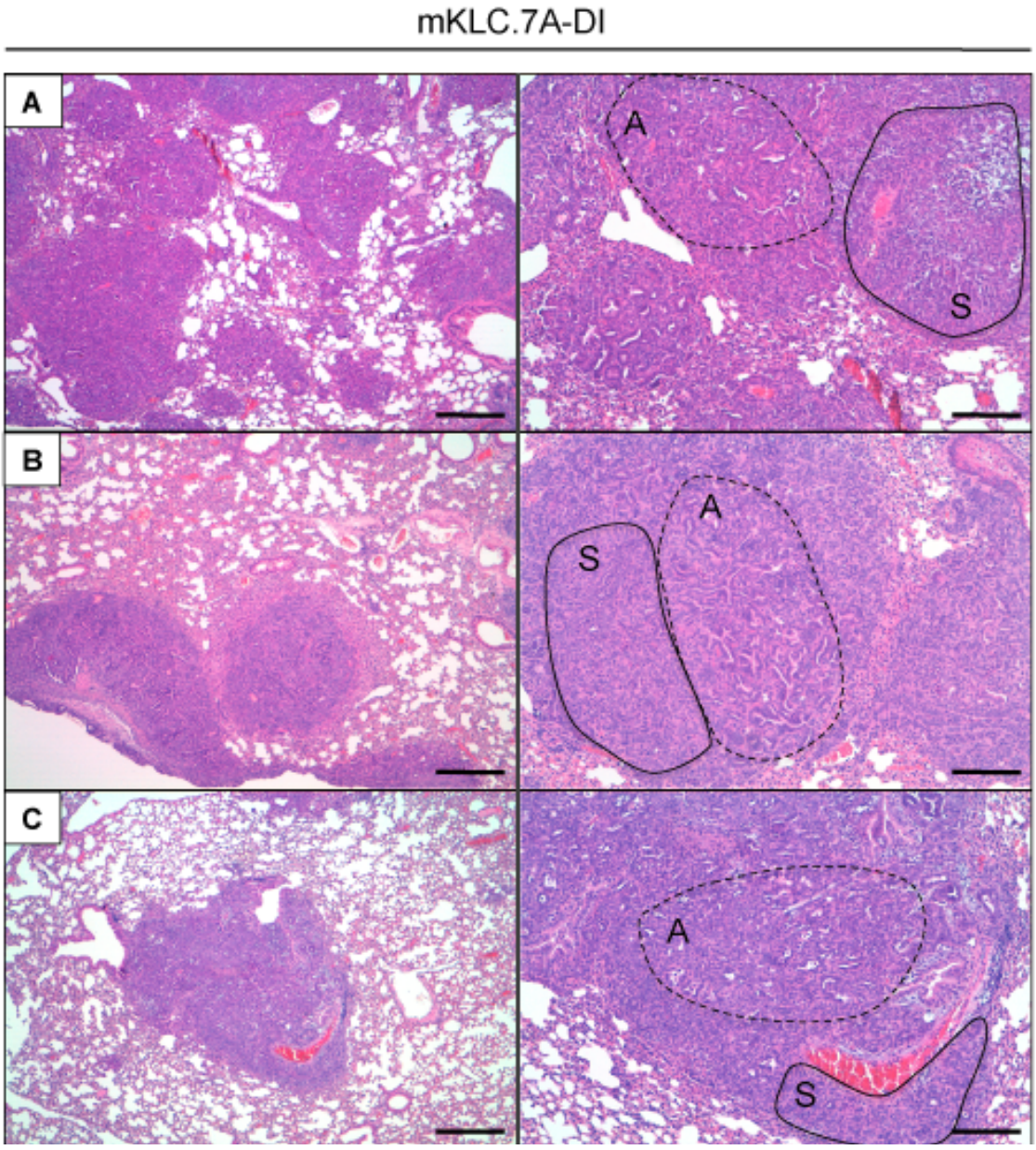

Fig. S4. Inoculation of mKLC single cell clones gives rise to NSCLC heterogeneity *in vivo.*

Representative H&E staining of lung tumors developed following tail vein injection of three independent cell lines **(A-C)** derived upon single cell cloning of mKLC.7A-DI. The presence of mixed solid (S) and acinar (A) histopathological component is indicated in the right panels. Scale bars 400 µm (left panels), 200 µm (right panels).